Dynamic agent of an injectable and self-healing drug-loaded hydrogel for embolization therapy

Xiaqing Zhou[a,1], Yongsan Li[b,c,1], Shuang Chen[a], Ya-nan Fu[b], Shihui Wang[b], Guofeng Li[b], Lei Tao[c], Yen Wei[c], Xing Wang[a,b,*], Jun F. Liang[a,*]

[a] Department of Chemistry and Chemical Biology, Charles V. Schaefer School of Engineering and Sciences, Stevens Institute of Technology, Hoboken, New Jersey 07030, USA
[b] Beijing Laboratory of Biomedical Materials, Beijing University of Chemical Technology, Beijing 100029, PR China
[c] The Key Laboratory of Bioorganic Phosphorus Chemistry & Chemical Biology (Ministry of Education), Department of Chemistry, Tsinghua University, Beijing 100084, PR China

ARTICLE INFO

ABSTRACT

Embolic agents are crucial for trans-catheter arterial embolization (TAE) in the treatment of various unresectable malignant tumors. Although solid particles, liquid oils, and some polymeric hydrogels have proved their capacities for embolic therapies, the low efficiency, time sensitivity, and cytotoxicity are still considered as challenges. In this study, we developed a three-component dynamic self-healing hydrogel to overcome these limitations. With the help of the Schiff-base bonding, both glycol-chitosan and carbazochrome, containing amine groups, react with dibenzaldehyde-terminated poly(ethylene-glycol) (DF-PEG), forming the dynamic self-healing hydrogels under a mild condition within 200 s. ^{1}H NMR and rheology test were used to characterize the Schiff-base formation and mechanical strength. Controlled-release of carbazochrome from different gelator concentrations of DF-PEG was also studied. Furthermore, *in vivo* evaluation of the embolization on rats showed the superior embolic effects of the injectable and self-healing hydrogel. Therefore, this new dynamic agent demonstrated the potential for application as a simple, inexpensive, and tunable embolic agent for cancer treatment and drug delivery system.

1. Introduction

Currently, various unresectable malignant tumors that present in the pancreas, liver, prostate, kidney, or brain have become a global burden to human health [1,2]. However, the appropriate managements and therapies to each of these types of cancer are still badly in need to alleviate patient pain and reduce the mortality rate. As a new and improved technique, trans-catheter arterial embolization (TAE) has been well developed as one of the safest methods with high efficiency in embolization cancer therapies and has been adopted in different tumor treatments worldwide with successes [3,4]. On one hand, TAE can not only preferentially interrupt the tumor's blood supply, but also stall growth until neovascularization [5]. On the other hand, focused administration of injecting embolic agents allows for specific delivery of an efficient dose of therapeutic compounds, such as chemotherapeutic drugs or hemostatic agents, while simultaneously avoiding systemic exposure which is considered as the limitation of dose usage [6,7].

Embolic agents play the crucial role both in the developing of TAE and the performance of the treatment [8]. Studies were made to explore the potential candidates from the category of solid embolic materials as well as liquid embolic materials [9]. Solid embolic materials including coils, collagen, gelatin sponges, sutures, and detachable balloons are not suitable when the target arteries have certain shape and dimensional requirements, leading to the transportation of such solid embolic materials to be unable to reach to the smaller arteriole branches [10–14]. Furthermore, 30% occupation rate of target arteries lumen is considered as another challenge in the application, which may cause the high recanalization and recurrence rates for patients and increase the risk on the secondary surgery [15]. In contrast, liquid embolic materials, such as Onyx® (ev3, Irvine, CA), poly(vinyl alcohol) (PVA), cellulose acetate polymer, and ethylene vinyl alcohol copolymer mixtures (EVAL), have been shown to achieve more complete fulfillment [16–18]. However, all of these agents are dissolved in organic solvents (*e.g.* dimethyl sulfoxide (DMSO)) and injected into target arteries. Some

serious complications and side effects such as infection, arterial rupture, and even death may occur owing to the cytotoxicity of the organic solvent [19–21]. Other concerns in the application of liquid embolic materials are that liquid materials are not resorbable and loadable; migration of the embolic agents also has the risk to trigger local or even systemic toxicity [22,23].

Improvements have been made recently by some hydrogels which are in between solid and liquid embolic materials, providing a promising candidate for embolization treatment [24–26]. Hydrogel is a soft substance with a very high water content and is composed of a cross-linked polymers. Hydrogels have been widely used in biomedical fields due to their significant similarity in structure and properties to human soft tissues [27]. Nguyen et al, developed a novel hydrogel system named PCLA-PUSSM for unresectable hepatocellular carcinoma treatment. The hydrogel is composed of biodegradable triblock poly(ε-caprolactone-co-lactide)-poly(ethyleneglycol)-poly(ε-caprolactone-co-lactide) copolymer and sulfamethizine [25]. Although this hydrogel system provides a potential chemoembolization candidate for cancer therapy, it still faces some challenges, including complicated preparation procedure and poor mechanical properties. Zhou et al, utilized graphene-oxide enhanced polymer hydrogel (GPH) as a promising embolic agent capable of treating cerebrovascular diseases and malignant tumors [26]. However, the surgeon is required to inject the GPH at a certain time before the hydrogel clogs the catheter. Moreover, the expensive and complex gelators limit large-scale fabrication and subsequent clinical application. Therefore, it is crucial to discover a novel hydrogel that can overcome the above problems.

Self-healing hydrogel is a smart, soft material, the damage of which can trigger an auto-repair process to regenerate an integral hydrogel [28,29]. This kind of hydrogel can heal itself under physiological conditions, being able to fit in the shape of a catheter during injection and resist breaks caused by the rough movement during transport, leading to improved utilization efficiency and decreased toxicity to normal tissues [30,31]. In addtion, self-healing hydrogel has been proven useful in many research areas, such as drug delivery, 3D cell culture, wound-healing and as a basic platform for the development of some organic-inorganic biological hybrids [32–35]. Yang et al, utilized self-healing hydrogel as drug carrier to increase the anticancer effect of Taxol [32]. Li et al, found out that the self-healing hydrogel was an ideal candidate to incubate functional cells or stem cells for cell therapy [33]. Herein, our group developed a three-component self-healing chitosan-based dynamic hydrogel (PCC hydrogel) using the biocompatible glycol-chitosan (GC), the carbazochrome, which is an anti-hemorrahagic, and dibenzaldehyde-terminated poly(ethylene-glycol) (DF-PEG) as the gelators. GC is generally nontoxic and bacteriostatic [36]. It has also been utilized as an embolic agent for arterial embolization applications [37]. Carbazochrome has been investigated as a

hemostatic agent resulting from its ability to interact with α-adrenoreceptors on the surface of platelets, causing the aggregation and adhesion of platelets in the blood to form a platelet plug, ceasing blood flow [38]. Benzaldehyde groups were chosen to modify PEG chain ends for the reason that they are quick to react with the amine groups on chitosan backbone and carbazochrome separately, forming the Schiff-base bond rapidly under a mild condition [39]. In other words, a well-defined biocompatible self-healing hydrogel network was established between GC, carbazochrome, and DF-PEG by the uncoupling and recoupling of the imine linkage in the Schiff-base cross-links. Moreover, the remarkable dynamic equilibrium of PCC hydrogel presents the potential tunable capability of controlled hemostatic release even during arterial embolization.

2. Experimental Section

2.1. Materials

Dibenzaldehyde-functionalized polymer (DF-PEG, $Mn \sim 4000 \, g \, mol^{-1}$) was synthesized following a procedure mentioned in the previous study [40]. Carbazochrome (Adrenochrome semicarbazone), Glycol-chitosan (Wako Pure Chemical Industries, 90% degree of deacetylation), N,N'-dicyclohexylcarbodiimide (DCC, Aladdin, 99%), 4-dimethylamiopryidine (DMAP, Aladdin, 99%), 4-formylbenzoic acid (99%) were used as purchased. Tetrahydrofuran (THF, 99.9%) was stored over sodium under a nitrogen atmosphere and distilled prior to use. Other reagents, if not mentioned, were all purchased from Sigma-Aldrich Company (St. Louis, MO, USA). Distilled water and 0.10 M phosphate buffer were used for solution preparation.

2.2. Measurements

All ^1H Nuclear Magnetic Resonance (NMR) spectra were recorded on a Varian 400 MHz spectrometer (Palo Alto, California). All ultraviolet-visible spectra were carried out on a Perkin-Elmer LAMBDA 35 UV/vis system. Rheology analyses were performed on a TA-AR2000ex rheometer. The weight measurements were made with a Discovery DV114C electronic analytic balance (Ohaus Corporation, NJ, U.S.A).

2.3. Preparation of the hydrogels

The carbazochrome-containing chitosan-PEG hydrogel (PCC) were prepared *via* Schiff-base bonding reactions at room temperature as shown in Scheme 1. In brief, the chitosan solution was firstly prepared by dissolving glycol-chitosan (0.033 g) in a saline solution (0.9% NaCl, 1000 μL). Afterwards, 200 μL of carbazochrome solution (3.2 mg/mL) was added into chitosan solution, followed by triturating 20–30 times
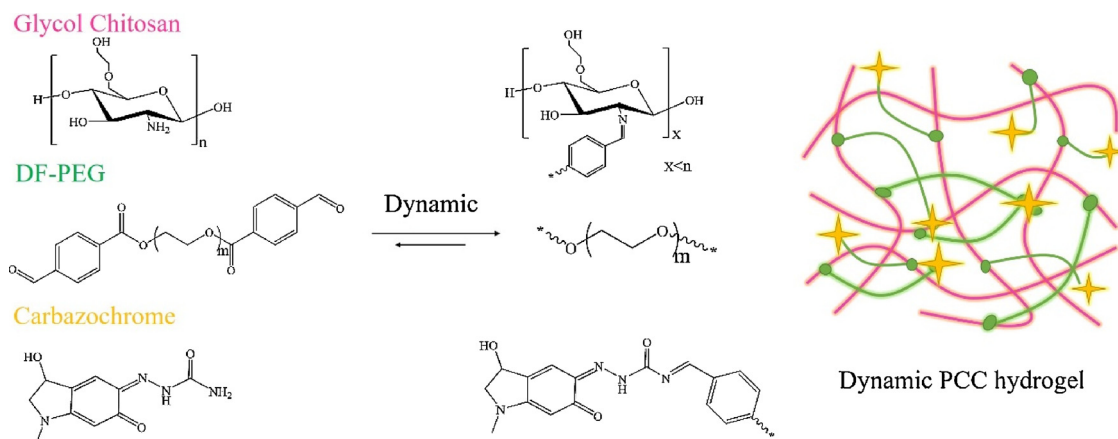
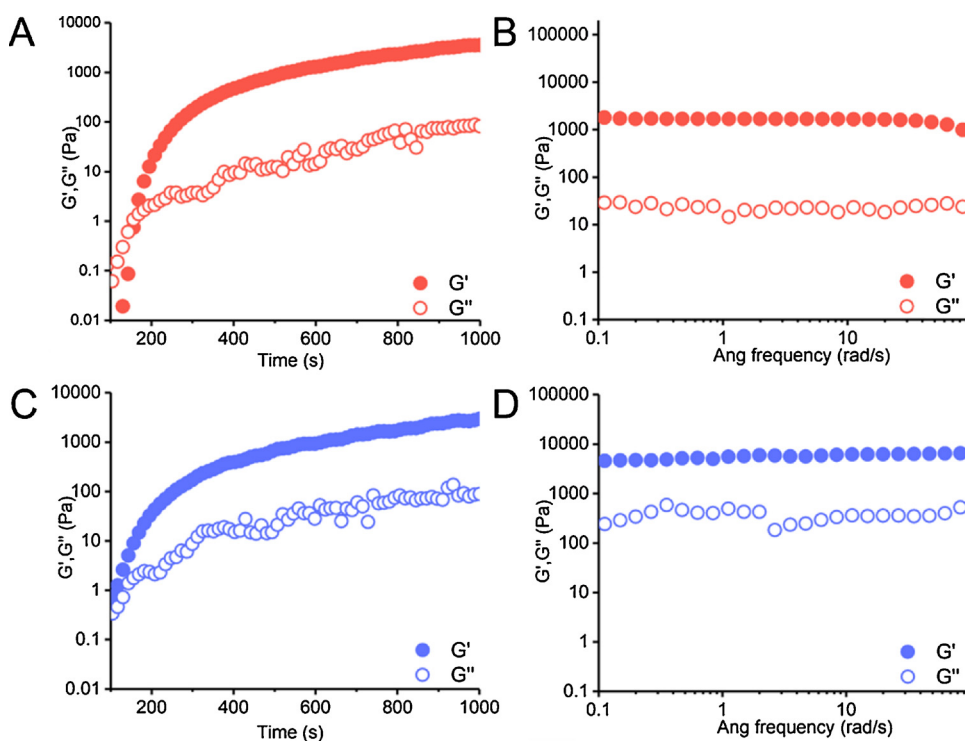**Scheme 1.** Synthesis of carbazochrome-containing chitosan-PEG hydrogel (PCC).

to evenly distribute the drug. Then, DF-PEG solution (1000 μL) with different concentration 5 wt% or 10 wt% was added respectively to generate a transparent carbazochrome-containing hydrogel for further research. ^{1}H NMR (Figure S1) technique was used in the characterization of the Schiff-base formation between PCC.

2.4. Rheology test

Rheometer was used to characterize the hydrogel's mechanical properties. Hydrogels with different concentration of DF-PEG were prepared and subjected to the rheology test. As a typical operation, glycol-chitosan solution with carbazochrome (0.2 g) was spread on the parallel plate of the rheometer. Then, DF-PEG aqueous solution (0.2 g, 5 wt% /10 wt%) was evenly added dropwise onto the chitosan solution surface and quickly mixed with a pipette tip. Storage moduli G′ and loss moduli G″ were measured as a function of time. In addition, storage modulus and loss modulus *versus* frequency analyses were carried out using a steel plate (diameter: 20 mm) and performed at 1% strain and 6.3 rad s^{-1}.

2.5. Qualitative self-healing experiment

An injection experiment was conducted in order to evaluate the PCC hydrogel's self-healing ability. In brief, the dynamic 5 wt% and 10 wt% PCC hydrogels were prepared in two separate syringe barrels by mixing the glycol-chitosan solution, carbazochrome solution, and the DF-PEG solution together (dyes were added for easy observations, red: 5 wt% PCC hydrogel; blue: 10 wt% PCC hydrogel). Then, these two hydrogels were extruded directly through 28-gauge needles into Eppendorf tubes, respectively.

2.6. Quantitative self-healing experiment

Continuous step changes in the oscillatory strain between 200% and 1% under the same frequency (1.0 Hz) were applied to test the self-healing ability of the PCC hydrogel with different concentration of DF-PEG. The profile of The G′ values to different amplitude were subsequently carried out. The shear thinning was induced *via* application of

200% strain for 2 min, afterwards, the strain was decreased to 1% for another 2 min to allow the gel to recover. The process was repeated twice.

2.7. Carbazochrome drug release

In vitro release studies of carbazochrome from 5 wt% and 10 wt% PCC hydrogels were conducted using a UV–vis spectrometer. Typically, the carbazochrome loaded hydrogels (1.0 mL) were prepared in a 15 mL centrifuge tube and the same volume of saline solution was added as the release media. At a predetermined time interval (from 0.1 h to 6 h), 1 mL sample solution was taken out to analyze the release amount of carbazochrome, while 1 mL of saline solution was replaced in the centrifuge tube for successive release. The release system was kept in a 37 °C incubator to mimic the *in vivo* release environment. Afterwards, the drug release experiments were repeated in triplicate and the OD values were plotted *versus* incubation time.

2.8. In vivo embolization

All animal experiments were performed in compliance with technical guidelines for non-clinical study of cytotoxic anti-tumor drugs issued by CFDA. Male SD rats, approximately 7 weeks old (average body weight of 200 g), were raised in quarantine for 1 week in a standard environment prior to the operation. The rats were randomly divided into three groups (3 rats each group) and marked as: Control group, PC hydrogel group (100 μL chitosan + 100 μL 10 wt% DF-PEG), PCC hydrogel group (100 μL chitosan + 100 μL 10 wt% DF-PEG + 20 μL carbazochrome). The PCC and PC hydrogels were prepared and injected into the renal arteries of the targeted kidneys after anaesthetizing the rats with pentobarbital (2 wt%, 0.1 mL). All rats were sacrificed on the 7th day, and the kidneys were excised for further analysis.

2.9. Histology

The rats' kidney samples for histologic analysis from *in vivo* culture were collected and fixed in freshly prepared 37% formaldehyde fixative for 1 h prior to processing and embedding. Fixed tissue specimens were
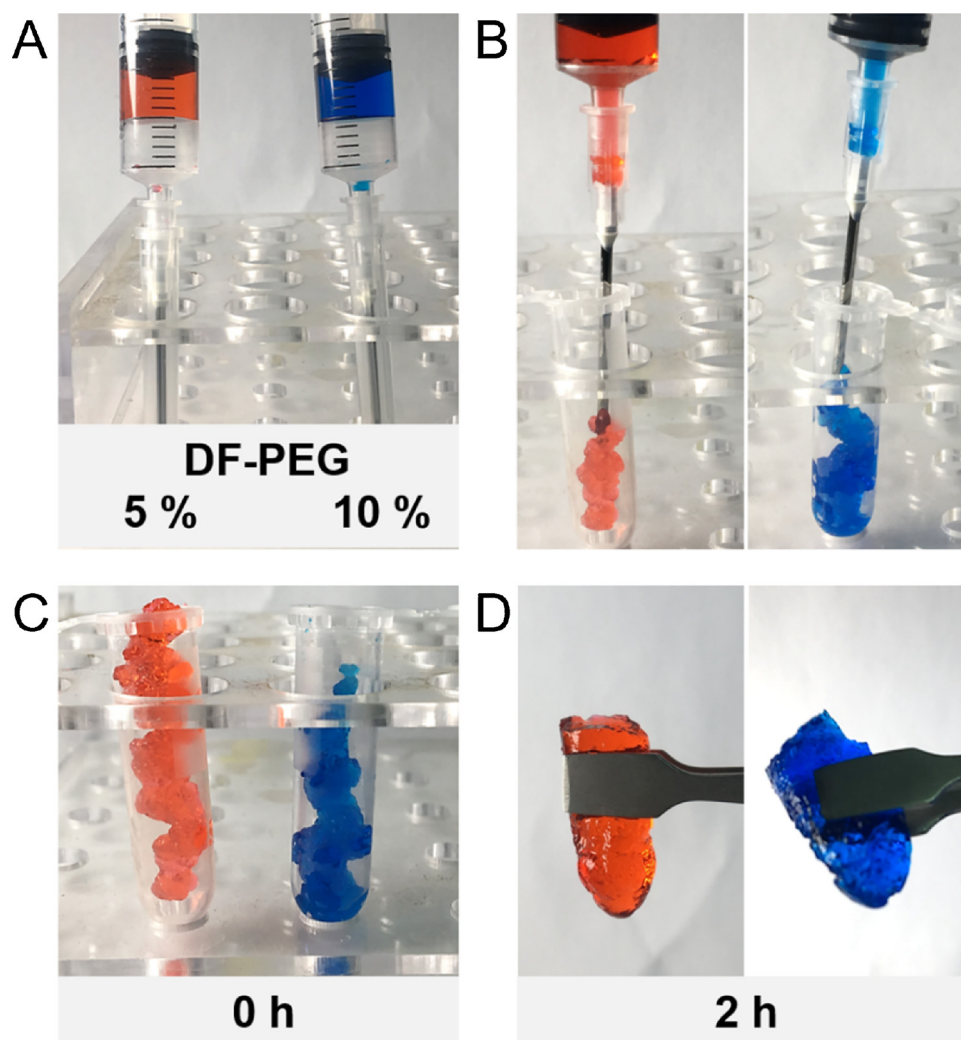
Fig. 2. Pictures of the 5 wt% PCC hydrogel (Red) and 10 wt% PCC hydrogel (Blue) (A) loaded in syringe; (B) start injecting; (C) just injected; (D) after 2 h (for interpretation of the references to colour in the figure legend, the reader is referred to the web version of this article).
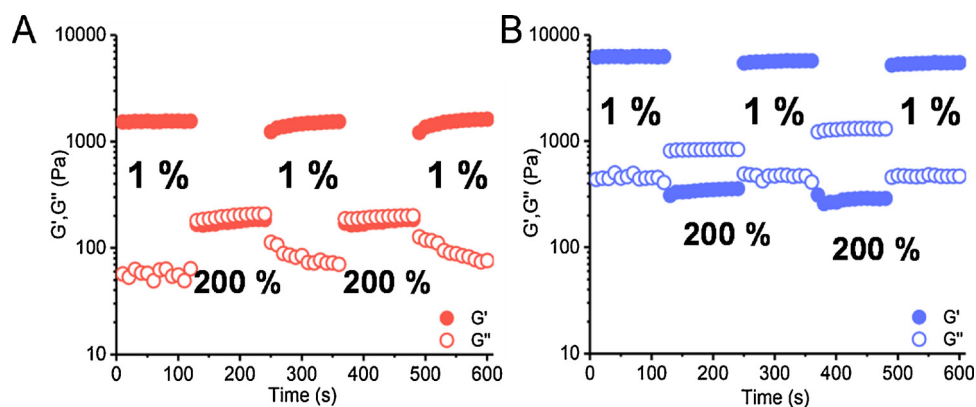

Fig. 3. The self-healing property of hydrogels demonstrated by the continuous step strain measurements: (A) 5 wt% PCC hydrogel; (B) 10 wt% PCC hydrogel.

dehydrated in a series of gradient ethanol solutions until 100% ethanol. The dehydrating agent was then cleared by incubation in xylene prior to paraffin embedding. Paraffin was heated to 60 °C and then allowed to harden overnight. Subsequently, the tissue were cut into thin sections (~10 μm thick). All specimens were then stained with hematoxylin and eosin (H&E). The stained slides were examined under a Nikon Eclipse 80i light microscope, and representative images were digitally documented.

3. Results and discussion

3.1. Rheology analysis of the gelation process

Two PCC hydrogels with different moduli were prepared using the same wt% of chitosan and carbazochrome, however, with different concentrations of DF-PEG (5%, 10%). Dynamic rheology was performed to investigate the mechanical properties of these hydrogels. As shown in
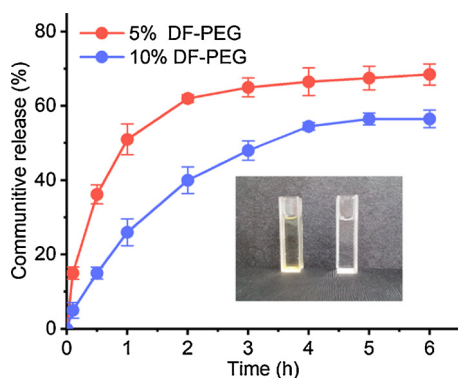
Fig. 4. The carbazochrome release profile of the 5 wt% (red) and 10 wt% (blue) PCC hydrogel at pH = 7.4 saline solution. Insert, carbazochrome (left) or none-carbazochrome (right) loaded 10 wt% PCC hydrogels (for interpretation of the references to colour in the figure legend, the reader is referred to the web version of this article).

Fig. 1A and C, the storage modulus (G′) surpassed the loss modulus (G″) immediately, typically, G′ surpassed the G″ in about 200 s for 5 wt% PCC hydrogel (red color) and about 100 s for 10 wt% PCC hydrogel (blue color), demonstrating the rapid crosslinking process for both hydrogels. However, based on the above results, PCC hydrogel with 10 wt% DF-PEG exhibited quicker formation of hydrogel than PCC hydrogel with 5 wt% DF-PEG. The frequency sweep in Fig. 1B and D shows that 5 wt% and 10 wt% PCC hydrogels exhibited a typical solid-like rheological behavior with the elastic moduli (G′, ~1.7 kPa for 5 wt% PCC hydrogel; ~5.7 kPa for 10 wt% PCC hydrogel) which demonstrated the viscous moduli G″ over the investigated frequency range. The enhanced gel strength of 10 wt% PCC hydrogel (G′ of 10 wt% PCC hydrogel is about 3 times larger than that of 5 wt% PCC hydrogel) could be directly linked to the increase of higher cross-linking density, resulting in greater stiffness. As expected, the higher storage modulus value was observed with the higher wt% DF-PEG.

3.2. Qualitative self-healing experiment

Since the PCC hydrogel network is constructed by Schiff base, the transient linkages between GC, carbazochrome, and DF-PEG predict that the chains in the hydrogel network will undergo de-crosslinking and re-crosslinking continuously. Therefore, after being injected by a syringe, the hydrogel should be deformed under shear stress and restored to a complete hydrogel when the stress is relieved. To test that, an injection experiment was conducted to evaluate the self-healing property of both 5 wt% and 10 wt% PCC hydrogels qualitatively. As shown in Fig. 2A and 2B, these two hydrogels were loaded in two separate syringes and then squeezed out through a 28-guage needle into an Eppendorf tubes, respectively. After that, the PCC hydrogels were kept in a 37 °C incubator to mimic the in vivo condition. For both 5 wt% and 10 wt% PCC hydrogels, the broken hydrogel pieces regenerated an entire piece of gel within 2 h (Fig. 2C and D), demonstrating the excellent self-healability of the PCC hydrogels with different concentration of DF-PEG.

3.3. Quantitative self-healing experiment

Continuous step change of oscillatory strain between 200% and 1% under the same frequency (1.0 Hz) was carried out to quantitatively monitor the self-healing process of both 5 wt% and 10 wt% PCC hydrogels. In brief, the profile of G′ and G″ values to different amplitudes was shown in Fig. 3A and B. Structure destruction of the hydrogel was triggered through the application of 200% strain for 2 min, and then the strain was reduced to 1% for another 2 min to allow the gel to recover. For the 5 wt% PCC hydrogel, the 200% strain decreased the G′ of the self-healing hydrogel from ~1.1 kPa to ~110 Pa. The G′ below G″ indicated the break-down of the hydrogel network. Then, when elevating the shearing force, the G′ of the self-healing hydrogel was returned quickly to ~1.1 kPa which is close to the initial value under the 1% strain, demonstrating the restore of the inner structure. Meanwhile, similar phenomenon was observed for the 10 wt% PCC hydrogel. As the strain value being raised to 200%, the G′ value was decreased from 6.0 kPa to 200 Pa. However, the G′ recovered quickly to the initial value after decreasing the amplitude to 1%, indicating a sol-to-gel transition. These results supported the self-healing ability of both 5 wt% and 10 wt% PCC hydrogels. Thus, the hydrogel could be considered as promising injectable matrials.

3.4. Cumulative release of carbazochrome

Quantitative analyses of carbazochrome released under 5 wt% and 10 wt% PCC were subsequently tested using a UV–vis spectrometer at 350 nm [41]. Cumulative release of carbazochrome in vitro is displayed in Fig. 4. Briefly, the carbazochrome loaded hydrogels were prepared and immersed in saline solution and kept at 37 °C. The release percentage of carbazochrome from 10 wt% PCC was approximately 50% in the first four hours with a rather slow continuing release to reach a total cumulative release of around 56% after 6 h. Compared with 10 wt% PCC, the release behavior of carbazochrome from 5 wt% PCC hydrogel was also studied. The results of 5 wt% PCC indicated that carbazochrome released much faster and 50% of carbazochrome was released in the first hour and up to 70% at the experiment's end. The difference in cumulative release between two hydrogels was due to the concentration of DF-PEG, indicating that the higher the concentration of DF-PEG, the lower the drug release rate. Increasing the concentration of DF-PEG would enhance the crosslink density of the hydrogel and make the network more compact. Therefore, the release of drugs would be limited, leading to longer release time.
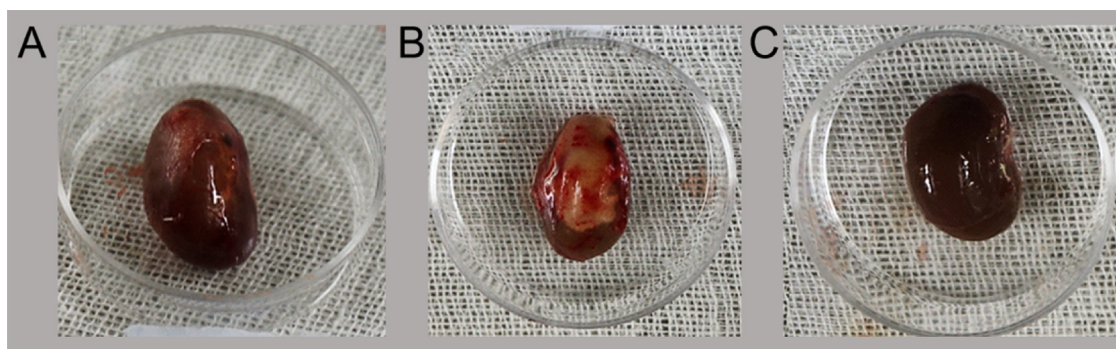

Fig. 5. Anatomopathological observation in rat kidney after hydrogel renal artery injection 7 days. Macroscopic photographs represent PCC hydrogel group (A), PC hydrogel group (B) and Control group (C) respectively.
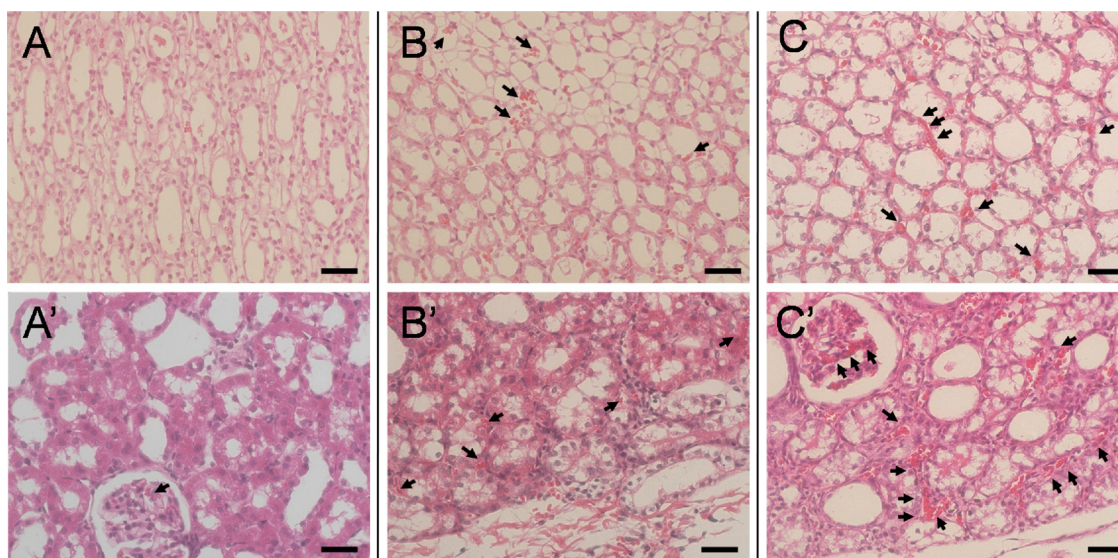
Fig. 6. Hematoxylin and eosin (H&E) - stained kidney sections of rats after 7 days *in vivo* culturing from different groups: (A) Control Group from Medulla; (A') Control Group from Cortex; (B) PC Group from Medulla; (B') PC Group from Cortex; (C) PCC Group from Medulla; (C') PCC Group from Cortex. (Black solid arrows indicate the embolization, 40X, Scale bar: 30 μm).

3.5. In vivo tests

Basing on the above results, 10 wt% PCC hydrogel was selected for the animal expeiments because 10 wt% PCC hydrogel has quicker gel formation and slower drug release comprared with 5 wt% PCC hydrogel. In brief, PC hydrogel and PCC hydrogel with 10 wt% DF-PEG were respectively applied to the *in vivo* rat's renal artery injection experiments to evaluate the embolization effects after 7 days. Rat renal model is a well-established animal model for evaluating embolic materials because of its readily available comparison (right kidney and left kidney) [37]. The rat has two kidneys. One kidney can be used as a control group, and one kidney is used as an experimental group to be injected with the embolic agent. In this case, it is easy to compare the morphology of the two kidneys after the experiments. In addition, The rat kidney model is more economical and effective than culturing the tumor model, for example a human liver cancer tumor (BEL-7402). For parallel comparison, a normal rat's kidney without any treatment, was set and harvested as the control group. Anatomopathological observations were made after kidneys were excised and shown in Fig. 5. The rats' kidney swelling as well as changes of blood volume, resulting in macroscopic color variance, were observed in both PC hydrogel and PCC hydrogel groups when compared with the control group. The causes were believed as the hydrogel injection, which blocked the renal arteries blood supply and limited the nutrition available at the target site. However, in contrast to the PC hydrogel group, thrombosis that triggered by carbazochrome in PCC hydrogel led to a more uniform change in color and swelling of the kidney which was caused by slow release of loaded carbazochrome in the PCC hydrogel.

3.6. Histology images of kidney slices

To further determine the embolization effect in between different groups, the tissue sections were subjected to hematoxylin and eosin staining and illustrated in Fig. 6. Mild pathological changes were identified in the PC group by the appearance of necrotic renal tubule cells as well as renal glomerulus cells in medulla or cortex in contrast with the control group. Additionally, more significant histological changes were discerned by the increasing orange-stained areas, indicating the necrosis and degeneration of individual cells caused by renal ischemia. Compared with the PC group, larger areas of embolization were formed in PCC hydrogel group because of carbazochrome

which was cumulatively released and transported. Both cell necrosis observed in the PC and PCC groups proved the embolization made by Schiff-base hydrogel system after renal injection. Moreover, the losing of integrated cell structure and increasing continues necrosis area in the PCC hydrogel group further demonstrated superior embolization effect of the cumulative releasing of carbazochrome.

4. Conclusion

In this study, three-component dynamic self-healing hydrogels with 5 wt% and 10 wt% concentrations of DF-PEG were contracted. The introducing of the Schiff-base bondings in the 3D hydrogel network endowed the self-healing ability and excellent mechanical properties. By means of uncoupling and recoupling of imine linkage in the Schiff-bass cross-links, an inexpensive, simple, biocompatible, and rapid method to prepare embolic self-healing hydrogel was exhibited by using GC, carbazochrome, and DF-PEG as gelators. The effects of different concentrations of DF-PEG on controlled carbazochrome release were found, leading to the tunable decomposition of the hydrogels. *In vivo* animal test and histology study proved that the three-component hydrogels were able to aid in rapid targeted embolization. The dynamic self-healing PCC hydrogel system is easy available, relatively low cost, low risk, and shows good control over position during embolization compared with multiple embolic agents. Futhermore, the accurate and controllable size forming and gelation make it possible to form the intended shape and complete distal migration. The work demonstrates that the composite dynamic self-healing PCC hydrogel system might be a promising candidate for embolization therapy.

Conflict of interests

The authors declare no competing financial interest.

Acknowledgments

Appendix A. Supplementary data

Supplementary material related to this article can be found, in the online version, at doi:https://doi.org/10.1016/j.colsurfb.2018.09.016.

References

[1] M. Ezzati, A.D. Lopez, A. Rodgers, S. Vander Hoorn, C.J. Murray, Selected major risk factors and global and regional burden of disease, Lancet 360 (2002) 1347–1360.

[2] J. He, D. Gu, X. Wu, K. Reynolds, X. Duan, C. Yao, J. Wang, C.S. Chen, J. Chen, R.P. Wildman, M.J. Klag, P.K. Whelton, Major causes of death among men and women in China, N. Engl. J. Med. 353 (2005) 1124–1134.

[3] H. Jiang, Q. Meng, H. Tan, S. Pan, B. Sun, R. Xu, X. Sun, Antiangiogenic therapy enhances the efficacy of transcatheter arterial embolization for hepatocellular carcinomas, Int. J. Cancer 121 (2007) 416–424.

[4] A. Rammohan, J. Sathyanesan, S. Ramaswami, A. Lakshmanan, P. Senthil-Kumar, U.P. Srinivasan, R. Ramasamy, P. Ravichandran, Embolization of liver tumors: past, present and future, World J. Radiol. 4 (2012) 405–412.

[5] Z.W. Peng, Y.J. Zhang, M.S. Chen, L. Xu, H.H. Liang, X.J. Lin, R.P. Guo, Y.Q. Zhang, W.Y. Lau, Radiofrequency ablation with or without transcatheter arterial chemoembolization in the treatment of hepatocellular carcinoma: a prospective randomized trial, J. Clin. Oncol. 31 (2013) 426–432.

[6] Y. Harima, T. Shiraishi, K. Harima, S. Sawada, Y. Tanaka, Transcatheter arterial embolization therapy in cases of recurrent and advanced gynecologic cancer, Cancer 63 (1989) 2077–2081.

[7] D.P. Harrington, K.H. Barth, R.R. Baker, B.T. Truax, M.D. Abeloff, R.I. White Jr., Therapeutic embolization for hemorrhage from locally recurrent cancer of the breast, Radiology 129 (1978) 307–310.

[8] Y.X. Wang, T. De Baere, J.M. Idee, S. Ballet, Transcatheter embolization therapy in liver cancer: an update of clinical evidences, Chin. J. Cancer Res. 27 (2015) 96–121.

[9] S. Vaidya, K.R. Tozer, J. Chen, An overview of embolic agents, Semin. Intervent. Radiol. 25 (2008) 204–215.

[10] J.V. Byrne, M.J. Sohn, A.J. Molyneux, B. Chir, Five-year experience in using coil embolization for ruptured intracranial aneurysms: outcomes and incidence of late rebleeding, J. Neurosurg. 90 (1999) 656–663.

[11] F. Brassel, D. Meila, Evolution of embolic agents in interventional neuroradiology, Clin. Neuroradiol. 25 (Suppl 2) (2015) 333–339.

[12] S. Miyayama, K. Yamakado, H. Anai, D. Abo, T. Minami, H. Takaki, T. Kodama, T. Yamanaka, H. Nishiofuku, K. Morimoto, T. Soyama, Y. Hasegawa, K. Nakamura, T. Yamanishi, M. Sato, Y. Nakajima, Guidelines on the use of gelatin sponge particles in embolotherapy, J. Radiol. 32 (2014) 242–250.

[13] T.J. Masaryk, J. Perl 2nd, R.C. Wallace, M. Magdinec, D. Chyatte, Detachable balloon embolization: concomitant use of a second safety balloon, Am. J. Neuroradiol. 20 (1999) 1103–1106.

[14] J. Théron, P. Courtheoux, A. Casasco, F. Alachkar, Local intraarterial fibrinolysis in the carotid territory, Risk Factors, Imaging of Brain Metabolism Spine and Cord Interventional Neuroradiology Free Communications, Springer, Berlin Heidelberg, 1989 303-303.

[15] T. Ries, C. Groden, Endovascular treatment of intracranial aneurysms: long-term stability, risk factors for recurrences, retreatment and follow-up, Klin. Neuroradiol. 19 (2009) 62–72.

[16] D.F. Vollherbst, C.M. Sommer, C. Ulfert, J. Pfaff, M. Bendszus, M.A. Mohlenbruch, Liquid embolic agents for endovascular embolization: evaluation of an established (Onyx) and a novel (PHIL) embolic agent in an in vitro AVM model, Am. J. Neuroradiol. 38 (2017) 1377–1382.

[17] D.B. Brown, T.K. Pilgram, M.D. Darcy, C.E. Fundakowski, M. Lisker-Melman, W.C. Chapman, J.S. Crippin, Hepatic arterial chemoembolization for hepatocellular carcinoma: comparison of survival rates with different embolic agents, J. Vasc. Interv. Radiol. 16 (2005) 1661–1666.

[18] J. Hamada, Y. Kai, M. Morioka, K. Kazekawa, Y. Ishimaru, H. Iwata, Y. Ushio, A nonadhesive liquid embolic agent composed of ethylene vinyl alcohol copolymer and ethanol mixture for the treatment of cerebral arteriovenous malformations: experimental study, J. Neurosurg. 97 (2002) 889–895.

[19] G.J. Velat, J.F. Reavey-Cantwell, C. Sistrom, D. Smullen, G.L. Fautheree, J. Whiting, S.B. Lewis, R.A. Mericle, C.S. Firment, B.L. Hoh, Comparison of N-butyl cyanoacrylate and onyx for the embolization of intracranial arteriovenous malformations: analysis of fluoroscopy and procedure times, Neurosurgery 63 (2008) ONS73-78; discussion ONS78-80.

[20] F. Mottu, A. Laurent, D.A. Rufenacht, E. Doelker, Organic solvents for pharmaceutical parenterals and embolic liquids: a review of toxicity data, PDA J. Pharm. Sci. Technol. 54 (2000) 456–469.

[21] J.C. Chaloupka, D.C. Huddle, J. Alderman, S. Fink, R. Hammond, H.V. Vinters, A reexamination of the angiotoxicity of superselective injection of DMSO in the swine rete embolization model, Am. J. Neuroradiol. 20 (1999) 401–410.

[22] J.I. Bilbao, A. Martínez-Cuesta, F. Urtasun, O. Cosín, Complications of embolization, Semin. Intervent. Radiol. 23 (2006) 126–142.

[23] R. Regine, F. Palmieri, M.De Siero, A. Rescigno, V. Sica, R. Cantarela, V. Villari, Embolization of traumatic and non-traumatic peripheral vascular lesions with onyx, Interv. Med. Appl. Sci. 7 (2015) 22–29.

[24] L. Weng, N. Rostambeigi, N.D. Zantek, P. Rostamzadeh, M. Bravo, J. Carey, J. Golzarian, An in situ forming biodegradable hydrogel-based embolic agent for interventional therapies, Acta Biomater. 9 (2013) 8182–8191.

[25] Q.V. Nguyen, J.S. Lym, C.T. Huynh, B.S. Kim, H.J. Jae, Y.I. Kim, D.S. Lee, A novel sulfamethazine-based pH-sensitive copolymer for injectable radiopaque embolic hydrogels with potential application in hepatocellular carcinoma therapy, Polym. Chem. 7 (2016) 5805–5818.

[26] F. Zhou, L. Chen, Q. An, L. Chen, Y. Wen, F. Fang, W. Zhu, T. Yi, Novel hydrogel material as a potential embolic agent in embolization treatments, Sci. Rep. 6 (2016) 32145.

[27] S. Reitmaier, A. Shirazi-Adl, M. Bashkuev, H.-J. Wilke, A. Gloria, H. Schmidt, In vitro and in silico investigations of disc nucleus replacement, J. R. Soc. Interface 9 (2012) 1869–1879.

[28] D.L. Taylor, M. in het Panhuis, Self-healing hydrogels, Adv. Mater. 28 (2016) 9060–9093.

[29] Y. Li, X. Wang, Y. Wei, L. Tao, Chitosan-based self-healing hydrogel for bioapplications, Chin. Chem. Lett. 28 (2017) 2053–2057.

[30] X. Zhang, K. Wang, M. Liu, X. Zhang, L. Tao, Y. Chen, Y. Wei, Polymeric AIE-based nanoprobes for biomedical applications: recent advances and perspectives, Nanoscale 7 (2015) 11486–11508.

[31] D.S. Benoit, C.R. Nuttelman, S.D. Collins, K.S. Anseth, Synthesis and characterization of a fluvastatin-releasing hydrogel delivery system to modulate hMSC differentiation and function for bone regeneration, Biomaterials 27 (2006) 6102–6110.

[32] L. Yang, Y. Li, Y. Gou, X. Wang, X. Zhao, L. Tao, Improving tumor chemotherapy effect using an injectable self-healing hydrogel as drug carrier, Polym. Chem. 8 (2017) 5071–5076.

[33] Y. Li, Y. Zhang, F. Shi, L. Tao, Y. Wei, X. Wang, Modulus-regulated 3D-cell proliferation in an injectable self-healing hydrogel, Colloids Surf. B Biointerfaces 149 (2017) 168–173.

[34] Y. Li, X. Wang, Y.-n. Fu, Y. Wei, L. Zhao, L. Tao, Self-adapting hydrogel to improve the therapeutic effect in wound-healing, ACS Appl. Mater. Interfaces 10 (2018) 26046–26055.

[35] M. Liu, G. Zeng, K. Wang, Q. Wan, L. Tao, X. Zhang, Y. Wei, Recent developments in polydopamine: an emerging soft matter for surface modification and biomedical applications, Nanoscale 8 (2016) 16819–16840.

[36] L. Xu, X. Zhang, C. Zhu, Y. Zhang, C. Fu, B. Yang, L. Tao, Y. Wei, Nonionic polymer cross-linked chitosan hydrogel: preparation and bioevaluation, J. Biomater. Sci. Polym. Ed. 24 (2013) 1564–1574.

[37] L. Weng, P. Rostamzadeh, N. Nooryshokry, H.C. Le, J. Golzarian, In vitro and in vivo evaluation of biodegradable embolic microspheres with tunable anticancer drug release, Acta Biomater. 9 (2013) 6823–6833.

[38] M. Basile, S. Gidaro, M. Pacella, P.M. Biffignandi, G.S. Gidaro, Parenteral troxerutin and carbazochrome combination in the treatment of post-hemorrhoidectomy status: a randomized, double-blind, placebo-controlled, phase IV study, Curr. Med. Res. Opin. 17 (2001) 256–261.

[39] Y.N. Fu, Y. Li, G. Li, L. Yang, Q. Yuan, L. Tao, X. Wang, Adaptive chitosan hollow microspheres as efficient drug carrier, Biomacromolecules 18 (2017) 2195–2204.

[40] Y. Zhang, L. Tao, S. Li, Y. Wei, Synthesis of multiresponsive and dynamic chitosan-based hydrogels for controlled release of bioactive molecules, Biomacromolecules 12 (2011) 2894–2901.

[41] M. Mohamed Abdelrahman, E.A. Abdelaleem, N.W. Ali, R.A. Emam, Simultaneous determination of carbazochrome and troxerutin in their binary mixture by HPLC and HPTLC-densitometric methods, Bull. Faculty Pharm., Cairo Univ. 54 (2016) 67–75.